Journal of Applied Mathematics and Physics (ZAMP)
Vol. 34, January 1983

0044-2275/83/001051-14 $ 4.30/0

On three-dimensional fibrous flaws in unidirectional fibre reinforced elastic composites

A. P. S. Selvadurai, Dept. of Civil Engineering, Carleton University, Ottawa, Ontario K1S 5B6, Canada

1. Introduction

An unidirectional fibre reinforced composite essentially consists of an elastic matrix which is reinforced by a random or regular network of closely spaced aligned fibres. The elastic stress analysis of such composites can be performed by idealizing the material as a transversely isotropic elastic medium. The overall elasticity parameters associated with the transversely isotropic elastic idealization can be estimated by recourse to a theory of composite materials applicable to fibre strengthened solids. Examples of such estimates are given by Hashin and Rosen [1] and Hill [2]. Extensive reviews of studies in this area are given by Broutman and Krock [3], Garg et al. [4] and Christensen [5].

The study of fracture processes in such unidirectional fibre reinforced composites is of fundamental importance to their engineering design. The articles by Kelly [6], Sih [7], Backlund [8] and Selvadurai [9] clearly illustrate the various phenomena such as matrix micro-cracking, matrix yielding, crack formation, fibre pullout, fibre debonding, flaw bridging etc., which lead to fracture of unidirectional fibre reinforced composites. This paper examines the related problem of the stress concentration at a spheroidal flaw in such an unidirectional fibre reinforced composite (Fig. 1). The structure of the flaw is such that the unidirectional fibres exhibit continuity across the flaw surface. The continuous elastic fibres impose a displacement-dependent traction boundary condition at the flaw surface. The classical theory for transversely isotropic elastic materials is used to generate the elastostatic solution for the "bridged spheroidal flaw" problem. It is shown that when the composite is subjected to a uniform stress field along the fibre direction the stress concentration factor for the bridged flaw can be evaluated in explicit form. The influence of flaw bridging on the stress concentration at the spheroidal flaw is illustrated by appeal to a specific unidirectional fibre reinforced solid with variable fibre volume fraction, fibre-matrix modular ratio and flaw geometry.

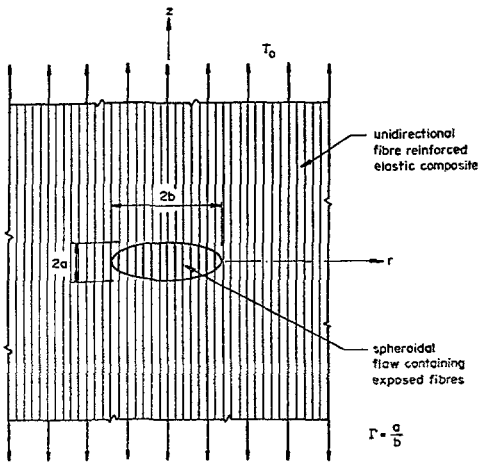

Figure 1
Geometry of the bridged spheroidal flaw in an unidirectional fibre reinforced composite.

2. Fundamental formulae

We consider the class of torsionless axisymmetric problem related to a transversely isotropic elastic medium in which the z-axis of the cylindrical polar coordinate system (r, θ, z) coincides with the axis of material symmetry. It can be shown (Elliott [10], Shield [11] and Chen [12]) that the displacement stress fields in the transversely isotropic elastic medium can be expressed in terms of two functions $\varphi_\alpha(r, z)$ $(\alpha = 1, 2)$ which are solutions of

$$\left(\frac{\partial^2}{\partial r^2} + \frac{1}{r}\frac{\partial}{\partial r} + \frac{\partial^2}{\partial z_\alpha^2}\right)\varphi_\alpha(r, z) = 0 \tag{1}$$

where $z_\alpha = z/n_\alpha^{1/2}$ and n_α are roots of the characteristic equation

$$c_{11}c_{44}n^2 + \{c_{13}(2c_{44} + c_{13}) - c_{11}c_{33}\}n + c_{33}c_{44} = 0. \tag{2}$$

In (2) c_{ij} are the elastic constants of the transversely isotropic elastic idealization of the unidirectional fibre reinforced solid. These constants can be expressed in terms of the isotropic elastic constants of the fibre (suffix f) and matrix (suffix m) phases and their respective volume fractions. (i.e. E_f, ν_f; E_m, ν_m and V_f, V_m respectively). These expressions are given by Hashin and Rosen [1]; a summary of the relevant results is also given in Appendix A.

The roots of (2) may be real or complex or both depending upon the elastic constants c_{ij} (see e.g. Elliott [10], Chen [12] and Kassir and Sih [13]). The displacement and stress fields in the transversely isotropic elastic material can be expressed in terms of $\varphi_\alpha(r, z)$ in the following forms.

$$\{u_r(r, z); u_z(r, z)\} = \sum_{\alpha=1}^{2}\left\{\frac{\partial\varphi_\alpha}{\partial r}; \frac{k_\alpha}{\sqrt{n_\alpha}}\frac{\partial\varphi_\alpha}{\partial z_\alpha}\right\} \tag{3}$$

$$\sigma_{rr} = c_{44} \sum_{\alpha=1}^{2} \left[\frac{(1+k_\alpha)}{n_\alpha} \left\{ \frac{\partial^2}{\partial r^2} + \frac{1}{r}\frac{\partial}{\partial r} \right\} \varphi_\alpha - \frac{(c_{11}-c_{12})}{c_{44}} \frac{1}{r}\frac{\partial \varphi_\alpha}{\partial r} \right] \tag{4}$$

$$\sigma_{\theta\theta} = c_{44} \sum_{\alpha=1}^{2} \left[\frac{(1+k_\alpha)}{n_\alpha} \left\{ \frac{\partial^2}{\partial r^2} + \frac{1}{r}\frac{\partial}{\partial r} \right\} \varphi_\alpha - \frac{(c_{11}-c_{12})}{c_{44}} \frac{\partial^2 \varphi_\alpha}{\partial r^2} \right] \tag{5}$$

$$\sigma_{zz} = c_{44} \sum_{\alpha=1}^{2} \frac{\partial^2 \varphi_\alpha}{\partial z_\alpha^2} \tag{6}$$

$$\sigma_{rz} = c_{44} \sum_{\alpha=1}^{2} \left\{ \frac{(1+k_\alpha)}{\sqrt{n_\alpha}} \frac{\partial^2 \varphi_\alpha}{\partial r \, \partial z_\alpha} \right\} \tag{7}$$

where

$$k_\alpha = \frac{c_{11} n_\alpha - c_{44}}{(c_{13} + c_{44})}; \quad (\alpha = 1, 2). \tag{8}$$

3. Boundary conditions

Before attempting to derive any specific solutions for $\varphi_\alpha(r, z)$ it is instructive to examine the boundary conditions that are applicable to the flaw bridging problem posed in the introductory paragraphs. For ease of reference, the displacement and stress components pertaining to the fibre and composite regions are denoted by the superscripts "f" and "c" respectively. The axial displacement of the independent fibres in the flaw region is denoted by $u_z^f(r, z)$ and the axial displacement in the unidirectionally reinforced composite region is denoted by $u_z^c(r, z)$.

The boundary ∂B of the spheroidal flaw region is described by the equation

$$\frac{z^2}{a^2} + \frac{r^2}{b^2} = 1 \tag{9}$$

where a und b are the semiaxes of the spheroidal flaw region. At the boundary ∂B there is continuity of displacement in the axial (z) direction. i.e.

$$u_z^f(r, z) = u_z^c(r, z) \quad \text{on} \quad (r, z) \in \partial B. \tag{10}$$

For continuity of surface traction in the axial direction (T_z) on this boundary we require

$$T_z^f(r, z) = T_z^c(r, z) \quad (r, z) \in \partial B. \tag{11}$$

Since the flexible elastic fibres that bridge the flaw region can exert tractions only in the axial direction it is evident that

$$T_r^c(r, z) = 0 \quad (r, z) \in \partial B. \tag{12}$$

Finally, the unidirectional fibre reinforced composite containing the bridged spheroidal flaw is subjected to a uniaxial state of stress which acts along the fibre (z) direction. At sufficiently large distances (denoted by region E) from the bridged flaw the state of stress is uniaxial. i.e.

$$\sigma^c_{zz}(r,z) = T_0 \quad (r,z) \in E \tag{13}$$

and all other $\sigma^c_{ij} = 0$.

4. Analysis of the bridged flaw problem

Composite Region

In the analysis of the bridged flaw problem it is convenient to represent the state of displacement and stress in the unidirectional fibre reinforced composite region as a combination of two separate solutions. The first corresponds to a uniaxial state of stress prescribed at infinity. The second solution (indicated by an asterisk) accounts for the presence of the bridged spheroidal flaw. The displacement and stress fields derived from the two solutions can be written in the forms

$$u^c_r(r,z) = -\frac{T_0 c_{13} r}{\chi} + u^*_r(r,z) \tag{14a}$$

$$u^c_z(r,z) = \frac{T_0 (c_{11} + c_{12}) z}{\chi} + u^*_z(r,z) \tag{14b}$$

and

$$\sigma^c_{rr}(r,z) = \sigma^*_{rr}(r,z) \tag{15a}$$

$$\sigma^c_{\theta\theta}(r,z) = \sigma^*_{\theta\theta}(r,z) \tag{15b}$$

$$\sigma^c_{zz}(r,z) = T_0 + \sigma^*_{zz}(r,z) \tag{15c}$$

$$\sigma^c_{rz}(r,z) = \sigma^*_{rz}(r,z) \tag{15d}$$

where

$$\chi = [c_{33}(c_{11} + c_{12}) - 2c^2_{13}] \tag{15e}$$

respectively.

To determine the displacement and stress fields u^*_i and σ^*_{ij} we employ a new variable $q(r,z)$ which is defined by the equation

$$\frac{z^2}{q^2} + \frac{r^2}{q^2 - 1} = c^2 \tag{16}$$

where

$$c^2 = a^2 - b^2. \tag{17}$$

The surface $q = \text{const.}$ represents a spheroid in the (r, z) space. The functions $q_\alpha(r, z_\alpha)$, $(\alpha = 1, 2)$ are defined by the relationships

$$\frac{z_\alpha^2}{q_\alpha^2} + \frac{r^2}{q_\alpha^2 - 1} = c_\alpha^2 \quad (\alpha = 1, 2) \tag{18}$$

where

$$c_\alpha^2 = a_\alpha^2 - b^2; \quad a_\alpha^2 = a^2/n_\alpha. \tag{19}$$

Also, when

$$q_\alpha = \varrho_\alpha; \quad \varrho_\alpha^2 = \frac{\Gamma^2}{\Gamma^2 n_\alpha}; \quad \Gamma = \frac{a}{b} \tag{20}$$

equation (18) reduces to the equation of the spheroidal flaw boundary ∂B defined by (9). Since the displacement and stress fields defined by u_i^* and σ_{ij}^* should reduce to zero at infinity, the potential functions $\varphi_\alpha(r, z)_\alpha$ are chosen to be of the form [12]

$$\varphi_\alpha(r, z) = \frac{A_\alpha}{2}[z_\alpha^2 \Psi_1(q_\alpha) + r^2 \Psi_2(q_\alpha) - c_\alpha^2 \Psi_0(q_\alpha)] \tag{21}$$

where

$$\Psi_0(q_\alpha) = \frac{1}{2}\log_e\left\{\frac{q_\alpha + 1}{q_\alpha - 1}\right\} \tag{22a}$$

$$\Psi_1(q_\alpha) = \frac{1}{2}\log_e\left\{\frac{q_\alpha + 1}{q_\alpha - 1}\right\} - \frac{1}{q_\alpha} \tag{22b}$$

$$\Psi_2(q_\alpha) = -\frac{1}{4}\log_e\left\{\frac{q_\alpha + 1}{q_\alpha - 1}\right\} + \frac{q_\alpha}{2(q_\alpha^2 - 1)}. \tag{22c}$$

Substituting the expressions for $\varphi_\alpha(r, z)$ into equations (3)–(7) we obtain the following expressions for u_i^* and σ_{ij}^*:

$$\{u_r^*(r, z); u_z^*(r, z)\} = \sum_{\alpha=1}^{2} A_\alpha \left\{r \Psi_2(q_\alpha); \frac{k_\alpha z_\alpha}{\sqrt{n_\alpha}} \Psi_1(q_\alpha)\right\} \tag{23}$$

$$\sigma_{rr}^*(r, z) = c_{44} \sum_{\alpha=1}^{2} \left\{\frac{A_\alpha(1 + k_\alpha)}{n_\alpha}\left[2 \Psi_2(q_\alpha) + r \frac{d\Psi_2}{dq_\alpha}(q_\alpha) \frac{dq_\alpha}{d_r}\right] - \frac{(c_{11} - c_{12})}{c_{44}} A_\alpha \Psi_2(q_\alpha)\right\} \tag{24}$$

$$\sigma_{\theta\theta}^*(r, z) = c_{44} \sum_{\alpha=1}^{2} \left\{A_\alpha\left[\frac{(1 + k_\alpha)}{n_\alpha} - \frac{(c_{11} - c_{12})}{c_{44}}\right] \cdot \left[2 \Psi_2(q_\alpha) + r \frac{d\Psi_2}{dq_\alpha}(q_\alpha) \frac{dq_\alpha}{dr}\right]\right\} \tag{25}$$

$$\sigma_{zz}^{*}(r,z) = c_{44}\sum_{\alpha=1}^{2} A_\alpha(1+k_\alpha)\left[\Psi_1(q_\alpha) + z_\alpha \frac{d\Psi_1}{dq_\alpha}(q_\alpha)\frac{dq_\alpha}{dz_\alpha}\right] \tag{26}$$

$$\sigma_{rz}^{*}(r,z) = c_{44}\sum_{\alpha=1}^{2} \frac{A_\alpha(1+k_\alpha)}{\sqrt{n_\alpha}} z_\alpha \frac{d\Psi_1}{dq_\alpha}(q_\alpha)\frac{dq_\alpha}{dz_\alpha}. \tag{27}$$

In the above equations

$$\frac{dq_\alpha}{dr} = \frac{r}{q_\alpha(q_\alpha^2-1)D_\alpha^2}; \quad \frac{dq_\alpha}{dz_\alpha} = \frac{z_\alpha}{q_\alpha^3 D_\alpha^2} \tag{28}$$

and

$$D_\alpha^2 = \frac{r^2}{(q_\alpha^2-1)^2} + \frac{z_\alpha^2}{q_\alpha^4}; \quad (\alpha = 1,2). \tag{29}$$

Fibrous flaw region

The fibrous flaw region contained within the boundary ∂B is denoted by F. Since the bridging fibres in this flaw region are continuously distributed one dimensional elastic elements with independent mechanical action, the variation of axial displacement u_z^f in the flaw region takes the general form

$$u_z^f(r,z) = z\,S(r) \quad (r,z)\in F \tag{30}$$

where $S(r)$ is some arbitrary function. Also since the bridging fibres are incapable of sustaining radial and shear stresses (i.e. $\sigma_{rr}^f(r,z) = \sigma_{rz}^f(r,z) = 0$), the component of surface traction on ∂B in the z-direction takes the form

$$T_z^f(r,z) = E_f V_f S(r) n_z \quad (r,z)\in\partial B \tag{31}$$

where n_z is the direction cosine of the normal to the spheroidal interface ∂B or $q = \varrho$. It can be shown that

$$n_r = \frac{r}{(\varrho^2-1)D_0}; \quad n_z = \frac{z}{\varrho^2 D_0} \tag{32}$$

where

$$D_0^2 = \frac{r^2}{(\varrho^2-1)^2} + \frac{z^2}{\varrho^4}. \tag{33}$$

Continuity conditions

Using the expressions (14), (23) and (30) the interface condition (10) pertaining to the continuity of axial displacement can be expressed in the form

$$S(r) = \xi + \frac{T_0}{c_{44}}\sum_{\alpha=1}^{2}\frac{\lambda_\alpha k_\alpha}{n_\alpha}\Psi_1(\varrho_\alpha) \quad (r,z)\in\partial B \tag{34}$$

where λ_α are the normalized values of A_α given by

$$\lambda_\alpha = \frac{A_\alpha c_{44}}{T_0} \tag{35}$$

and

$$\xi = \frac{c_{44}(c_{11} + c_{12})}{[c_{33}(c_{11} + c_{12}) - 2c_{13}^2]}. \tag{36}$$

Also, using the expressions (15), (26), (27) and (31) the interface condition (11) relating to the compatibility of tractions in the z-direction can be expressed in the form

$$S(r) = \frac{T_0}{E_f V_f}\left\{1 - \sum_{\alpha=1}^{2} \lambda_\alpha (1 + k_\alpha) \Psi_2(\varrho_\alpha)\right\} \quad (r, z) \in \partial B. \tag{37}$$

Similary, the interface condition (12) related to the component of traction in the r-direction gives

$$\sum_{\alpha=1}^{2} \lambda_\alpha \left\{\frac{(1 + k_\alpha)}{n_\alpha} \Psi_1(\varrho_\alpha) - \frac{(c_{11} - c_{12})}{c_{44}} \Psi_2(\varrho_\alpha)\right\} = 0 \quad (r, z) \in \partial B. \tag{38}$$

The equations (34), (37) and (38) can now be solved to evaluate the constants λ_α. For example

$$\lambda_1 = \zeta \lambda_2 \tag{39}$$

where

$$\zeta = \frac{-\left[\frac{(1 + k_2)}{n_2} \Psi_1(\varrho_2) + \frac{(c_{11} - c_{12})}{c_{44}} \Psi_2(\varrho_2)\right]}{\left[\frac{(1 + k_1)}{n_1} \Psi_1(\varrho_1) + \frac{(c_{11} - c_{12})}{c_{44}} \Psi_2(\varrho_1)\right]} \tag{40}$$

and

$$\lambda_2 = \frac{(1 - \xi \Omega)}{\left[\Omega\left\{\frac{k_1}{n_1} \zeta \Psi_1(\varrho_1) + \frac{k_2}{n_2} \Psi_1(\varrho_2)\right\} + 2(1 + k_1)\zeta \Psi_2(\varrho_1) + 2(1 + k_2)\Psi_2(\varrho_2)\right]}. \tag{41}$$

This formally completes the analysis of the fibrous elastic flaw contained in a unidirectional fibre reinforced composite. Expressions for the displacement and stresses in the composite and fibre regions can be evaluated by making use of the relevant general expressions given previously.

For example, the circumferential stress at the equator of the composite is given by

$$\frac{\sigma_{zz}(r, 0)}{T_0} = 1 + \sum_{\alpha=1}^{2} \lambda_\alpha (1 + k_\alpha) \Psi_1(q_\alpha^0) \tag{42}$$

where, on the plane $z = 0$,

$$(q_\alpha^0)^2 = \frac{\Gamma^2 + \bar{r}^2 n_\alpha - n_\alpha}{\Gamma^2 - n_\alpha}; \qquad \bar{r} = \frac{r}{b} \geqq 1. \tag{43}$$

In general, the parameters k_α, n_α, λ_α and the functions $\Psi_\beta(q_\alpha)$ ($\beta = 1, 2$) can be real- or complex-valued or both depending upon the magnitudes of the elastic constants c_{ij}. Consequently, the distribution of axial stress σ_{zz} on the equatorial plane is given by the following result

$$\frac{\sigma_{zz}(r,0)}{T_0} = 1 + \mathrm{Re}\left\{\sum_{\alpha=1}^{2} \lambda_\alpha (1 + k_\alpha)\, \Psi_1(q_\alpha^0)\right\} \tag{44}$$

where Re denotes the real part of the expression.

5. Numerical results

In order to illustrate the influence of elastic flaw bridging on the stress concentration at the spheroidal flaw we evaluate the stress distribution at the equator $\sigma_{zz}(r, 0)$ defined by (44). The expressions for the elastic constants c_{ij}, expressed in terms of the elastic properties of the matrix and fibre phases, are defined in Appendix A. Certain material parameters are assigned the following values: $E_m = 4 \times 10^6$ lb/in^2, $\nu_f = 0.20$, $\nu_m = 0.35$. The elastic modulus of the fibre material is expressed as a multiple of the elastic modulus of the matrix i.e. $E_f = M^* E_m$. The specification of the volume fraction completes the description of the transversely isotropic elastic composite material. The geometry of the flaw is specified by the flaw aspect ratio $\Gamma = a/b$. Values of $\Gamma = 2$ and 1/2

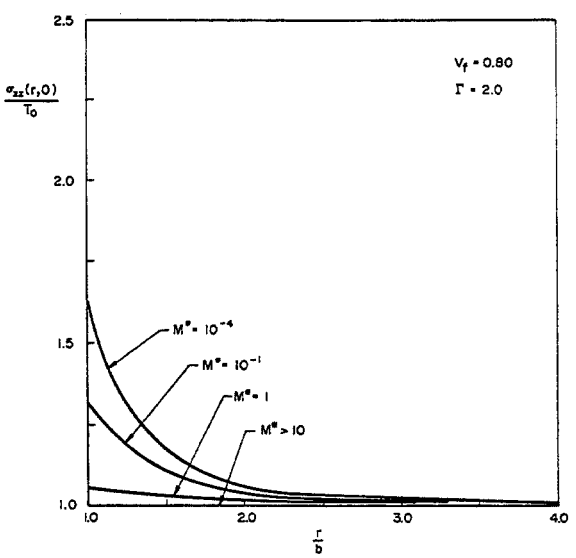

Figure 2
Variation of normal stress $\sigma_{zz}(r, 0)$ on the equatorial plane – prolate spheroidal flaw.

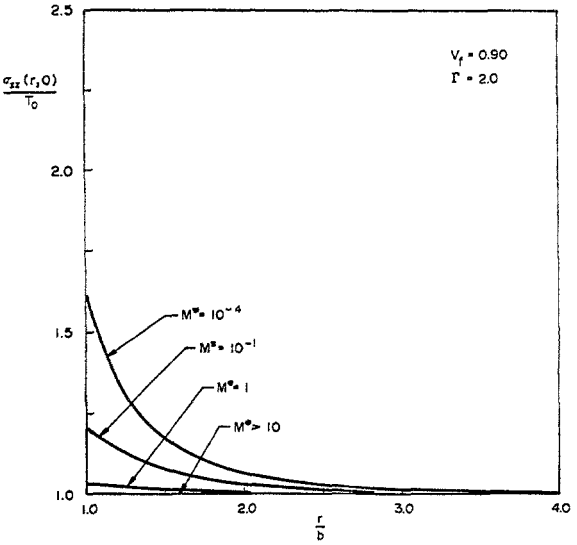

Figure 3
Variation of normal stress $\sigma_{zz}(r, 0)$ on the equatorial plane – prolate spheroidal flaw.

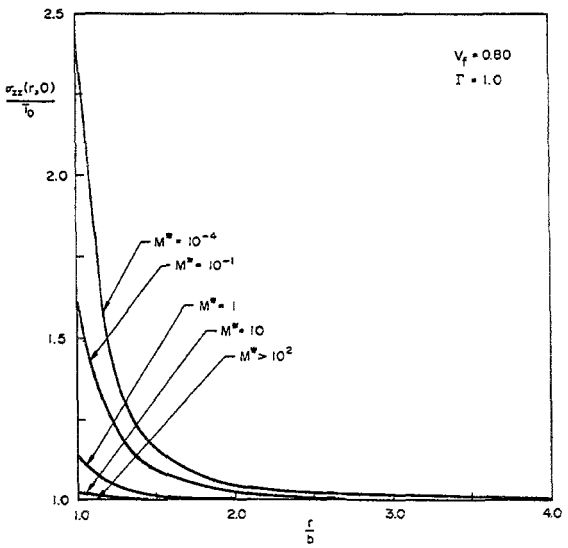

Figure 4
Variation of normal stress $\sigma_{zz}(r, 0)$ on the equatorial plane – spherical flaw.

correspond to spheroidal fibrous regions with prolate and oblate spheroidal shapes. $\Gamma = 1$ corresponds to a spherical fibrous flaw. In the numerical calculations, the real part of the function cited in equation (42) is evaluated by using a standard IML routine.

The Figures 2–7 illustrate the distribution of normal stress $\sigma_{zz}(r, 0)$ on the equatorial plane. These results indicate that the perturbations of the uniform stress field due to the bridged spheroidal flaw are restricted to the neighbourhood of the flaw. Also, the aspect ratio of the bridged spheroidal flaw Γ and the fibre-matrix modular ratio M^* has a significant influence on the magnitude and

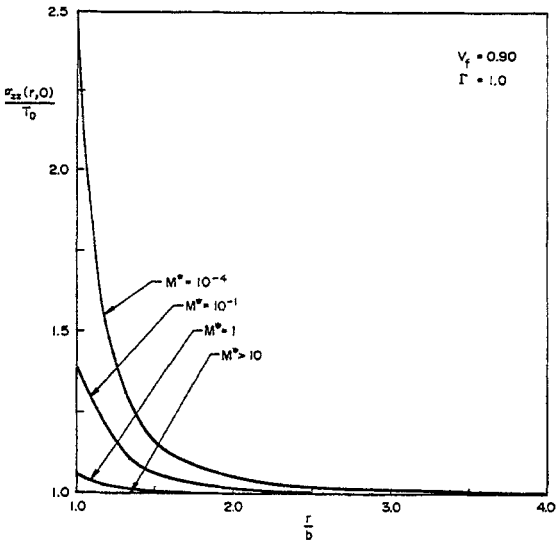

Figure 5
Variation of normal stress $\sigma_{zz}(r, 0)$ on the equatorial plane – spherical flaw.

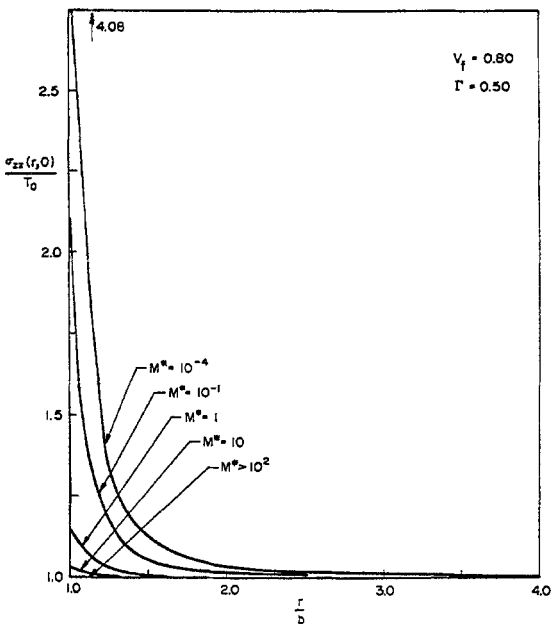

Figure 6
Variation of normal stress $\sigma_{zz}(r, 0)$ on the equatorial plane – oblate spheroidal flaw.

distribution of the normal stress $\sigma_{zz}(r, 0)$ on the plane of symmetry. The stress concentration factor $\sigma_{zz}(r, 0)/T_0$ increases as the aspect ratio Γ decreases. In the limit as $\Gamma \to 0$, the flaw resembles a bridged penny-shaped flaw. This limiting description of the bridged flaw as a spheroidal region is however much more realistic than the corresponding approximation in terms of a penny-shaped flaw (see e.g. Selvadurai, [9, 14]). In the limiting case as $\Gamma \to 0$ the stress concentra-

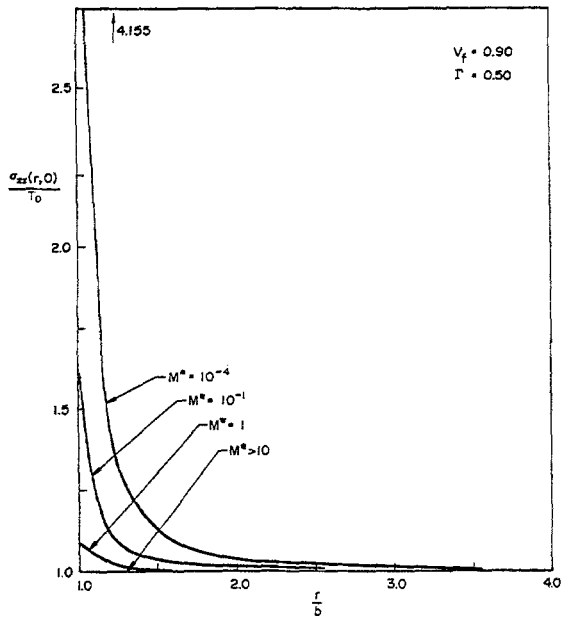

Figure 7
Variation of normal stress $\sigma_{zz}(r, 0)$ on the equatorial plane – oblate spheroidal flaw.

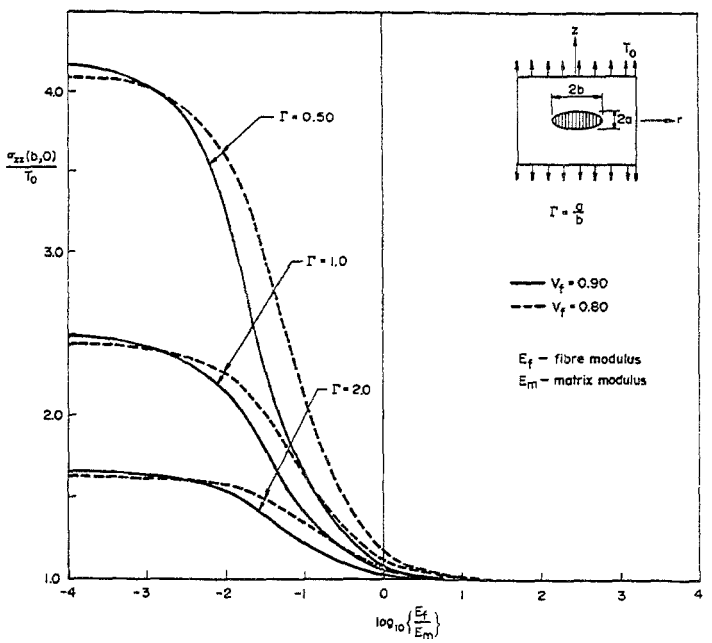

Figure 8
Influence of the fibre/matrix modular ratio on the stress concentration at the flaw boundary.

tion has to be examined as a stress intensity factor, $\lim_{r \to b^+} \sigma_{zz}(r, 0)$, to provide results of engineering interest to fracture mechanics.

The Figure 8 illustrates the influence of the modular ratio M^*, the volume fraction V_f and the aspect ratio Γ on the stress concentration at the boundary of the fibrous composite region. The modular ratio M^* has a marked influence on the axial stress concentration at the flaw boundary.

6. Conclusions

Studies in composite materials indicate that the continuity of fibres across a defect or flaw in a unidirectionally reinforced composite results in the development of elastic flaw bridging. This technologically important problem, however, has received only limited attention. In this paper we examine the stress analysis of a stable bridged spheroidal flaw in a unidirectional fibre reinforced composite. In particular, the paper develops a solution for the stress concentration in such a flaw which is subjected to a homogeneous stress field in the direction of the reinforcing fibres. The solution to the elastostatic stress analysis problem can be evaluated in compact form. Numerical results presented for the normal stress concentration on the equatorial plane indicate that the fibre-matrix elastic modular ratio of the composite has a significant influence on the stress concentration factor. As this modular ratio increases the bridging action diminishes the stress concentration factor. Such effects are of some significance to the development of fracture and failure at flaws occurring in fibre-reinforced materials.

Appendix A

The constants c_{ij} can be expressed in terms of the elastic constants E_i, ν_1, G_{23} and K_{23} (where the subscripts 1 refers to the fibre direction and the subscripts 2 and 3 refer to the transversely isotropic plane) in the form

$$c_{11} = K_{23} + G_{23}$$

$$c_{33} = E_1 + 4\nu_1^2 K_{23}$$

$$c_{13} = 2\nu_1 K_{23}$$

$$c_{12} = K_{23} - G_{23}$$

$$c_{44} = G_1 .$$

The relationships between E_1, ν_1, G_1 etc., and the properties of the fibre (f) and matrix (m) constituents (E_f, E_m, ν_f, ν_m) and the respective volume fractions

(V_f, V_m) are given below. The expression for G_{23} is equivalent to the upper bound for the assemblage, as found by Hashin and Rosen [1].

$$K_{23} = \left\{\frac{\zeta_0(1+2\nu_m V_f)+2\nu_m V_m}{\zeta_0 V_m + V_f + 2\nu_m}\right\}(\lambda_m + G_m)$$

$$G_{23} = G_m\left\{\frac{(\alpha+\beta_m V_f)(1+\varrho V_f^3)-3V_f V_m^2\beta_m^2}{(\alpha - V_f)(1+\varrho V_f^3)-3V_f V_m^2\beta_m^2}\right\}$$

$$\nu_1 = \left\{\frac{V_f E_f L_1 + V_m E_m L_2 \nu_m}{V_f E_f L_3 + V_m E_m L_2}\right\}$$

$$G_1 = G_m\left\{\frac{\eta(1+V_f)+V_m}{\eta V_m + V_f + 1}\right\}; \quad E_1 = V_f E_f + V_m E_m$$

where

$$L_1 = 2\nu_f(1-\nu_m^2)V_f + V_m\nu_m(1+\nu_m); \quad L_2 = 2V_f(1-\nu_f^2)$$

$$L_3 = 2(1-\nu_m^2)V_f + (1+\nu_m)V_m$$

$$\zeta_0 = \frac{\lambda_f + G_f}{\lambda_m + G_f}; \quad \alpha = \frac{\eta+\beta_m}{\eta-1}; \quad \varrho = \frac{\beta_m - \eta\beta_f}{1+\eta\beta_f}$$

$$\eta = \frac{G_f}{G_m}; \quad V_m + V_f = 1;$$

$$G_i = \frac{E_i}{2(1+\nu_i)}; \quad \lambda_i = \frac{\nu_i E_i}{(1+\nu_i)(1-2\nu_i)}; \quad \beta_i = (3-4\nu_i)^{-1}, \quad (i = m,f).$$

References

[1] Z. Hashin and B. W. Rosen, *The elastic moduli of fibre reinforced materials*, J. Appl. Mech., *31*, 223–232 (1964).

[2] R. Hill, *Theory of mechanical properties of fibre strengthened materials 1. Elastic behaviour*. J. Mech. Phys. Solids, *12*, 199–212 (1964).

[3] L. J. Broutman and R. H. Krock (Eds). Composite Materials Vols. 1–8, Academic Press, New York 1974.

[4] S. K. Garg, V. Svalbonas and G. A. Gurtman, Analysis of Structural Composite Materials, Marcel Dekker, New York 1973.

[5] R. M. Christensen, Mechanics of Composite Materials, John Wiley, New York (1979).

[6] A. Kelly, *Interface effects and the work of fracture of a fibrous composite*, Proc. Roy. Soc., Ser. A., *319*, 95–116 (1970).

[7] G. C. Sih, *Fracture mechanics of composite materials*, in Proc. 1st USA-USSR Symposium on Fracture of Composite Materials, (G. C. Sih and V. P. Tamuzs, Eds) Sijthoff and Noordhoff, The Netherlands, 113–130 (1979).

[8] J. Backlund, *Fracture analysis of notched composites*, Computers & Structures, *13*, 145–154 (1981).

[9] A. P. S. Selvadurai (Ed.), Mechanics of Structured Media: Studies in Applied Mechanics Vols. 5 A & 5 B, Proc. Int. Symp. Mech. Behaviour of Structured Media, Ottawa, Elsevier Scientific Publ. Co. Amsterdam 1981.

[10] H. A. Elliott, *Three dimensional stress distributions in hexagonal aeolotropic crystals*, Proc. Camb. Phil. Soc. *45*, 621–630 (1949).

[11] R. T. Shield, *Note on problems in hexagonal aeolotropic materials*, Proc. Camb. Phil. Soc., *47*, 401–409 (1951).
[12] W. T. Chen, *Axisymmetric stress field around spheroidal inclusions and cavities in a transversely isotropic material*, J. Appl. Mech. *35*, 770–773 (1968).
[13] M. K. Kassir and G. C. Sih, Three Dimensional Crack Problems. Mechanics of Fracture Vol. 2. (G. C. Sih, Ed.) Noordhoff Int. Publ. Co., The Netherlands 1975.
[14] A. P. S. Selvadurai, *Concentrated body force loading of an elastically bridged penny-shaped flaw in a unidirectional fibre reinforced composite.* Int. J. Fracture (1982) (in press).

Abstract

This paper examines the problem of the stress concentration at a flaw in a unidirectional fibre reinforced composite. The geometry of the flaw corresponds to a spheroidal region in which the reinforcing fibres exhibit continuity across the flaw surface. The composite containing the flaw is subjected to a uniaxial stress field which acts along the fibre direction. An exact solution is devoloped for the stress concentration factor at the reinforced flaw boundary. Typical numerical results presented in the paper illustrate the manner in which the stress concentration at the bridged flaw is influenced by the fibre volume fraction, the fibre-matrix modular ratio and the flaw geometry.

Zusammenfassung

In der vorliegenden Arbeit wird das Problem der Spannungskonzentration an einem Defekt in einem einachsig mit Fasern verstärkten Komposit untersucht. Der Defekt entspricht einem elliptisch-sphärischen Gebiet mit Fasern, welche durch die Defektfläche hindurch stetig verlaufen. Der Körper wird durch ein Spannungsfeld in Richtung der Fasern einachsig belastet. Ein exakter Lösungsansatz führt zum Spannungskonzentrationsfaktor an der Oberfläche des verstärkten Defektes. Typische numerische Resultate illustrieren den Einfluß des Volumen- und Modulverhältnisses zwischen Fasern und Matrix sowie der Defektgeometrie auf die Spannungskonzentration.

(Received: September 1, 1982)